Article

Design and Optimization of Power Shift Tractor Starting Control Strategy Based on PSO-ELM Algorithm

Yu Qian [1], **Lin Wang** [2] **and Zhixiong Lu** [1,*]

1 College of Engineering, Nanjing Agricultural University, Nanjing 210031, China; 2020212006@stu.njau.edu.cn
2 State Key Laboratory of Intelligent Agricultural Power Equipment, Luoyang 470139, China; wanglin@ytogroup.com
* Correspondence: luzx@njau.edu.cn

Abstract: Power shift tractors have been widely used in agricultural tractors in recent years because of their advantages of uninterrupted power during shifting, high transmission efficiency and high stability. As one of the indispensable driving states of the power shift tractor, the starting process requires a small impact and a starting speed that meets the driver's requirements. In this paper, aiming at such contradictory requirements, the starting control strategy of a power shift tractor is formulated with the goal of starting quality and the driver's intention. Firstly, the identification characteristics of the driver under three starting intentions are obtained by a real vehicle test. An extreme learning machine with fast identification speed and short training time is used to establish the basic driver's intention identification model. For the instability of the identification results of the Extreme Learning Machine (ELM), the particle swarm optimization algorithm (PSO) is used to optimize the ELM. The optimized extreme learning machine model has an accuracy of 96.891% for driver's intention identification. The wet clutch is an important part of the power shift gearbox. In this paper, the starting control strategy knowledge base of the starting clutch is established by a combination of bench tests and simulation tests. Through the fuzzy algorithm, the driver's intention is combined with the starting control strategy. Different drivers' intentions will affect the comprehensive evaluation model of the clutch (the single evaluation index of the clutch is: the maximum sliding power, the sliding power, the speed stability time, the impact degree), thus affecting the final choice of the starting clutch control strategy considering the driver's intention. On this basis, this paper studies and establishes the MPC starting controller for the power shift gearbox. Compared with the linear control strategy, the PSO-ELM-fuzzy weight starting strategy proposed in this paper can reduce the maximum sliding friction power by 45%, the sliding friction power by 69.45%, and the speed stabilization time by 0.11 s. The effectiveness of the starting control strategy considering the driver's intention proposed in this paper to improve the starting quality of the power shift tractor is verified.

Keywords: tractors; power shift transmission; starting process; driver's intention

1. Introduction

As the main tool of agricultural production, agricultural tractors often need to undertake field operations such as tillage, ploughing, sowing, and harvesting [1,2]. In addition, tractors also spend a large part of their time on road transportation [3,4]. Due to the changing working environment, the work of agricultural tractors is more complicated and demanding than that of road vehicles. Agricultural tractors can be divided into step transmission and stepless transmission according to their different transmission ratios. Stepped transmissions include manual mechanical shift transmission (MT), hydraulic torque converter transmission, dual clutch transmission (DCT) and power shift transmission (PST). Electric Continuously variable transmission (CVT), hydrostatic CVT and hydro-mechanical CVT [5–8]. At present, the development of tractors is moving from traditional manual

transmission and automatic transmission into newer transmission types, among which hydro-mechanical stepless transmission is a hot transmission. It combines the advantages of stepless speed regulation of the hydraulic system with the high efficiency of mechanical transmission so that the tractor can adapt to the changes in the external environment and make the engine work at its best. However, this transmission method has high requirements for manufacturing and control technologies such as shifting clutches and hydraulic control systems [9,10]. Electric continuously variable transmission is also composed of a power supply, control system and motor. The use of clean energy is friendly to the environment, but this transmission is subject to battery life [11].

The power shift transmission (PST) mainly relies on the sliding friction of the wet clutch to realize the shift without interrupting the engine power. Power shift technology solves the shortcomings of traditional mechanical gearbox parking shifts and power interruptions. Compared with the transmission mechanical shift tractor, the working efficiency of the power shift gearbox is increased by 10–20%. The power shift gearbox is divided into partial power shift and full power shift. The partial power shift is the main shift using wet clutch shift, and the auxiliary shift using electronically controlled synchronizer shift. Full power shift means all gears are wet clutch shift; this way, it requires a high-precision control system. In summary, the power shift gearbox has the advantages of high transmission efficiency, high reliability and high driving comfort and has an important position in agricultural tractors. Tanelli et al. [12] studied the shifting process and reversing process of the power shift transmission, and optimized the initial pressure of the clutch with the change in tractor speed during the shifting process as the optimization goal. Kim et al. [13] used computer simulation technology to explore the influence of the terminal pressure, forward speed, weight, shuttle gear ratio and torsional damping of the tractor on the shift performance of the power shift gearbox. As a result, the tractor weight increased the axle torque but had no effect on the power transmitted by the unit area of the clutch. Raikwar et al. [14] proposed a systematic methodology for the modeling and simulation of a power shuttle transmission system for agricultural tractors, which provides a more economical research method. Simulation is a time- and cost-effective method for the study of power shift transmission.

With the development of power shift technology, in order to meet the driver's increasing requirements for driving comfort and improve the stability of the tractor's shift or start under different working conditions, in the power shift gearbox, the electro-hydraulic control system gradually replaces the traditional mechanical shift control method. The electro-hydraulic control system refers to the pressure control and engagement and disconnection control of the wet clutch through the electro-hydraulic control valve, so as to complete the start and change control of the tractor. The electro-hydraulic control system has the advantages of fast response and high intelligence. In addition, it can be combined with an intelligent control algorithm to formulate a reasonable clutch control strategy according to different working conditions and engagement targets, so as to reduce the impact of tractor starting and section changing and improve the quality of tractor section changing and the driver's driving comfort [15].

As a key component of the power shift gearbox, the wet clutch is responsible for starting and shifting. Its engagement quality will directly determine the quality of the tractor during starting and shifting. The wet clutch uses oil pressure to push the piston, transmits torque through the friction between the friction plate and the steel plate, and performs the starting and shifting actions of the tractor. Ouyang et al. [16] established a wet clutch model that considered damping force, steady flow force and transient flow force to meet the requirements of precise control and fast response. Balau et al. [17] developed a linearized input-output model for an electro-hydraulic actuated clutch. Based on the model, a networked predictive controller was designed for the wet clutch with the aim of controlling the clutch piston displacement while decreasing the influence of the variable-time delays on the closed-loop control performances over the communication network. Zeng et al. [18] built a simulation model of a wet clutch hydraulic actuator system and

proposed a model-based feedforward and PID feedback control algorithm. Based on the dynamic equation of the wet clutch piston and proportional valve body and the flow equation of the hydraulic pump, Wu et al. [19] built a clutch oil filling simulation test platform to study the influence of PWM control signals with different rising rates on the clutch oil filling process.

The tractor is controlled by the driver when driving, and the driver controls the tractor according to different working environments and needs. When the tractor is in different conditions, the driver will have different driving needs. The research of Benloucif et al. [20], Marcano et al. [21] and Li et al. [22] also shows that the driver's intention is important in the future development of human–machine cooperative driving systems, so it plays an important role in the identification of the driver's intention. There are four types of driver's intentions during tractor driving: acceleration, deceleration, steering and lane change [23]. When the tractor starts from a stationary state, the driver's intention will have: slow start demand, general start demand, and rapid start demand.

The identification of the driver's intention first needs to determine the intention identification parameters. Liu et al. [24] simulated four types of drivers' intentions during vehicle driving: lane following, left lane change, right lane change and overtaking. The average number of fixations of the driver's left rearview mirror, the average head horizontal angle, the steering wheel angle, the longitudinal acceleration and the establishment of the center line of the vehicle and the lane are used as the driver's intention identification parameters. Wang et al. [25] used accelerator pedal opening, accelerator pedal opening change rate, vehicle average acceleration and vehicle speed to identify the driver's expected acceleration. For the identification model of the driver's intention, the identification models based on time series mainly include the k-nearest neighbor model, support vector regression, and artificial neural networks. However, due to the stochastic and nonlinear nature of behavior, they thus provide unsatisfying prediction performance [26]. Yao et al. [27] used the Hidden Markov identification model, and used the driving intention characteristic parameters after cluster analysis to iteratively optimize the identification model. Wang et al. [28] used the support vector machine model to establish the driver's intention identification model, which integrates vehicle operating parameters such as vehicle speed, environmental information and the driver's visual features.

At present, the research on power shift gearboxes is mostly concentrated in the fields of transmission scheme design and characteristic analysis, and there are few studies on starting control. With the increase in tractor use scenarios, tractors often stop and start again when they are working or transporting in the field. The impact of traditional tractors when starting is relatively high, which will have a great impact on the physical and mental health of agricultural machinery drivers who need to drive tractors for a long time. At the same time, research on the improvement of tractor starting quality in agricultural machinery is missing. The starting process of the power shift tractor is a process of 'human–machine–ground' interaction. The starting control considering the driver's intention will improve the starting quality of the tractor, which is of great significance to the performance improvement of the power shift gearbox. In this paper, the research goal is to improve the starting quality of the power shift tractor. Considering the driver's starting intention (starting demand), the optimal control strategy of the main starting part 'wet clutch' is studied.

The main contents of this paper are as follows:

(1) The identification parameters of the driver's starting intention and the classification of the driver's starting intention are determined by a real vehicle test. (2) The PSO algorithm is used to optimize ELM, and the identification model of the PST tractor driver's starting intention is established. (3) The bench test of clutch oil filling characteristics is carried out, and the knowledge base of the PST starting clutch control strategy is established. (4) In order to establish the comprehensive evaluation index of PST starting quality, fuzzy recognition is used to establish the mapping between the driver's starting intention and the weight of each engagement quality evaluation index in the starting clutch. (5) The PST starting simulation test platform is established, and the starting quality under the

starting control strategy proposed in this paper and the ordinary starting control strategy is compared based on the MPC controller. The purpose of this paper is to provide a theoretical basis for the formulation of a PST starting control strategy. This paper aims to improve the starting performance of a power shift tractor and the working comfort of agricultural machinery drivers.

2. Materials and Methods

2.1. Three Kinds of Driver Starting Intention Test

When the power shift tractor starts, the driver's actions mainly include stepping on the accelerator pedal and pushing the gear lever (starting gear: the power shift tractor generally starts at low speed). The driver's starting intention is generally divided into three types [29–32]. (1) Slow start. At this time, the driver steps on the accelerator pedal at a slower speed, hoping to start smoothly. (2) General start. At this time, the driver stampedes on the accelerator pedal speed in general, conventional starting speed and the starting time requirements in general; (3) Rapid start. The driver quickly steps on the accelerator pedal, and the change rate of the pedal opening is large. This starting mode has a higher requirement for the starting time. The depth of the driver's stampede on the accelerator pedal and the stampede speed are direct manifestations of the urgency of the start. At the same time, starting is a process of 'human–vehicle' interaction. The driver's different operations on the throttle will affect the response of the power shift tractor. The impact of the tractor is the most significant starting intention feedback index (where the impact is the first derivative of the longitudinal acceleration of the tractor). In summary, the accelerator pedal opening, the accelerator pedal opening change rate and the longitudinal acceleration are selected as the identification parameters of the driver's starting intention.

Let the experienced driver start the tractor at the test site. The tractor model used in the test is DF Ward 854 (China Jiangsu Changzhou Dongfeng Agricultural Machinery Group Co., Ltd., Changzhou, China) (Table 1). In order to measure the accelerator pedal opening signal and acceleration signal, the pedal opening sensor and acceleration sensor are installed on the tractor, Figure 1 shows the test process. A total of 60 groups of starting intention experiments were carried out (Figure 2), including 20 groups of slow starting intention, general starting intention and fast starting intention. The identification parameters under different starting intentions are obtained: throttle opening, throttle opening change rate and longitudinal acceleration.
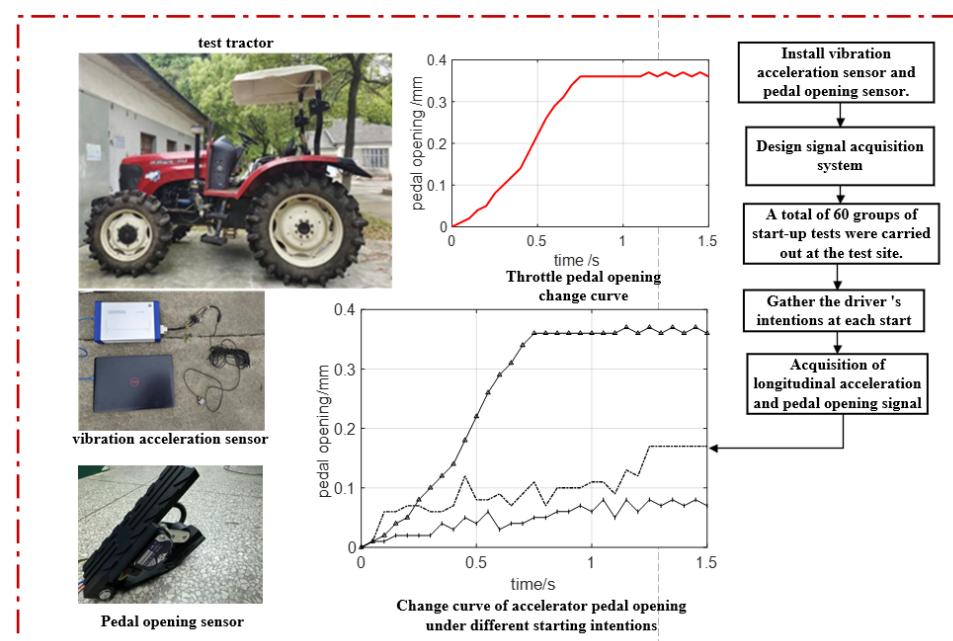

Figure 1. Driver's starting intention acquisition test.

Table 1. Comprehensive parameters of DF Wode 854 tractor.

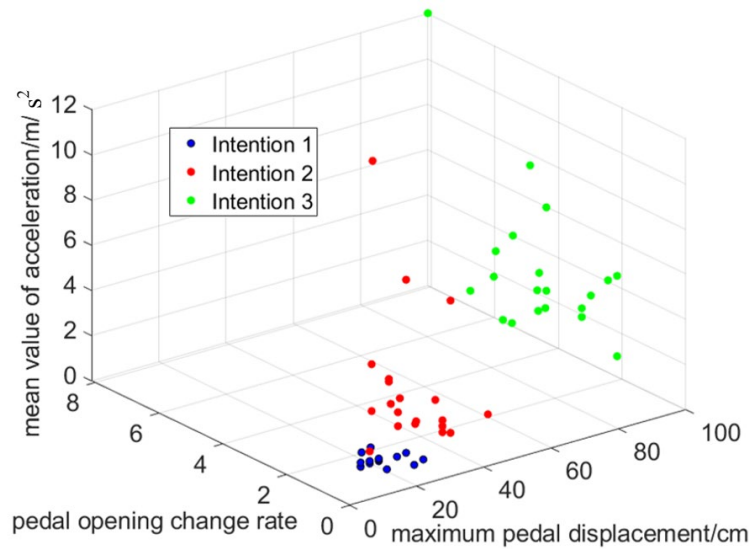| Parameter	Value
Power shift tractor machine type	Wheel
Weight (kg)	3570
Take-off output (kW)	$\geq$56.3
Rated tractive effect (kN)	$\geq$20
Rear cross member gauge (mm)	1620–2020
The working quality of whole machine (kg)	3800
Engine type	LRC4108T
Rated speed (r/min)	2300

Figure 2. Sixty sets of starting intention test data.

2.2. PSO Optimizes the ELM Identification Model of Driver's Starting Intention

2.2.1. ELM Identification Model

Extreme Learning Machine (ELM) is a single hidden-layer feedforward neural network composed of an input layer, a hidden layer and an output layer [33–35]. The essence of ELM is based on the linear solution process of random feature mapping, which can greatly reduce the complexity of the algorithm and improve the learning rate. Compared with the traditional neural network algorithm, which iteratively calculates and adjusts parameters to optimize the structure, the ELM algorithm is more suitable for the starting scene of the power shift tractor because of its short training time and small computational complexity.

The neural network model of ELM is shown in Figure 3. Input weight, output weight and threshold are used to establish the relationship between the two layers. Users can set the activation function and the number of hidden layer neurons. For Q group training data (X_i, Y_i), $X_i = [x_{i1}, x_{i2}, \ldots x_{in}] \in R^n, Y_i = [y_{i1}, y_{i2}, \ldots y_{im}] \in R^m$, L is the number of nodes in the hidden layer, $f(x)$ is the activation function. A single-layer feedforward network is modeled as follows.

$$\sum_{i=1}^{L} \beta_i f(w_i \cdot x_i + b_i), 1 \leq j \leq N \tag{1}$$

w_i is the weight between the input layer node and the ith hidden layer node. β_i is the weight between the ith hidden layer node and output layer node. b_i is the threshold of the ith hidden layer node. Q_j is the output of neural network. w_i, β_i and Q_j are vector values, $w_i = [w_{i1}, w_{i2}, \ldots w_{in}]^T$, $\beta_i = [\beta_{i1}, \beta_{i2}, \ldots \beta_{im}]^T$, $Q_j = [Q_{j1}, Q_{j2}, \ldots Q_{jn}]^T$. By learning the training data, the output value of the ELM model can approach the real value with faster speed and smaller error.

$$\sum_{i=1}^{L} \beta_i f(w_i \cdot x_i + b_i) = y_j, 1 \leq j \leq N \tag{2}$$

The output matrix of ELM is set to *H*, and the model can be rewritten as

$$H\beta = Y \tag{3}$$

H is the output value obtained from the Neural network. The learning goal of ELM is to minimize the output error. At this time, it can be solved by the least square method.

$$\left\| H\hat{\beta} - Y \right\| = \frac{min}{\beta} \| H\beta - Y \| \tag{4}$$

The optimal value of *β* obtained by matrix operation is

$$\hat{\beta} = H^{\dagger}T \tag{5}$$

In the formula, $H^{\dagger}$ is the generalized inverse matrix of matrix *H*.
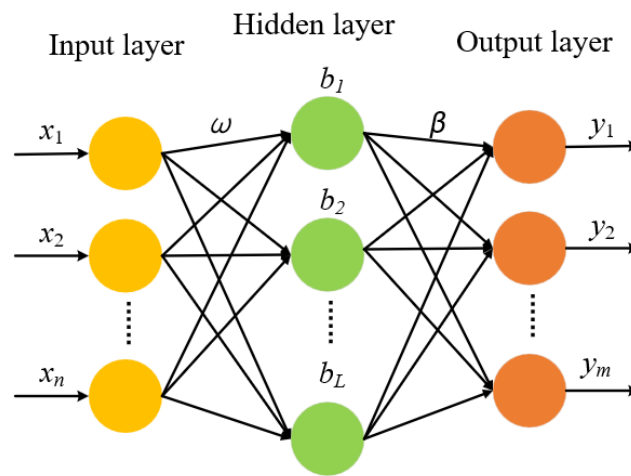

Figure 3. Extreme learning machine neural network model.

Based on the ELM algorithm, the driver's starting intention identification model is constructed. The number of hidden layer nodes is selected to be 100, and the sigmoid function is selected as the activation function. The expression is:

$$sig(x) = \frac{1}{1 + e^{-x}} \tag{6}$$

2.2.2. PSO-ELM Identification Model

In the particle swarm optimization algorithm model, the particles continuously optimize the target through the sharing and updating of group information. The particle velocity, position calculation formula and update formula [36–38] are:

$$V_t = \omega_s \bullet V_{t-1} + c_1 r_1 (p_{best} - x(t)) + c_2 r_2 (g_{best} - x(t))$$

$$\omega_s = \omega_{st} - (\omega_{st} - \omega_{en}) * \frac{K}{T} \tag{7}$$

Formula (7) is the particle update formula, V_t is the velocity of the particle at the next moment, ω_s is the inertia weight, V_{t-1} is the velocity of the particle at this time, c_1 and c_2 are individual learning factor and social learning factor, respectively. r_1 and r_2 are two unequal numbers in [0, 1], respectively. p_{best} is the historical optimal position of the particle, and g_{best} is the group optimal position. $x(t)$ is the position of the particle at this time, ω_{st} is the initial inertia weight of the particle, ω_{en} is the final inertia weight after the iteration is completed, *K* is the current number of iterations, and *T* is the total number of iterations. The variable inertia weight is introduced. In the early stage of iteration, the inertia weight of

individual particles is large, which makes the particles have strong exploration abilities. As the iteration progresses, the inertia weight of the individual particles gradually decreases, so that the particles quickly fly to the global optimal solution.

The input weights of the ELM algorithm are randomly generated by the system, and there is a certain instability. In this paper, the PSO algorithm is used to optimize the input weights of the ELM identification model. The particle swarm optimization algorithm has the advantages of strong versatility and fast convergence speed. For the study of drivers' starting intention recognition in this paper, the application scenarios that need faster recognition speed are more matched. The algorithm optimization flow chart of the particle swarm optimization algorithm to optimize the ELM model is shown in Figure 4:
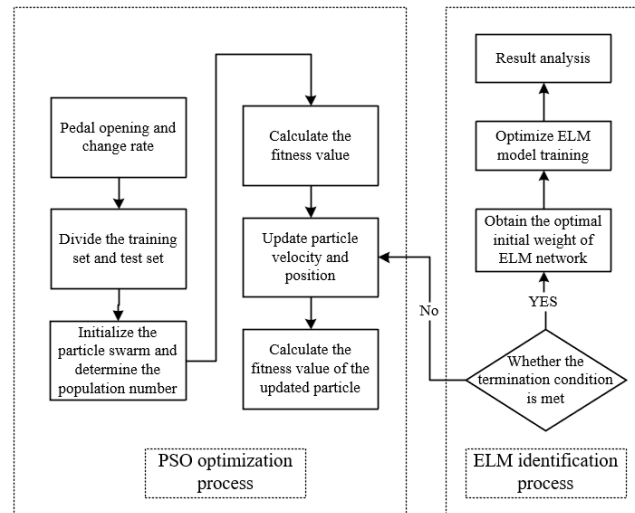

Figure 4. The flow chart of ELM optimized by PSO algorithm.

2.3. The Formulation of Clutch Control Strategy under Different Driving Intentions

2.3.1. Weight Determination of Starting Quality Evaluation Index Based on Fuzzy Recognition

The evaluation of clutch engagement quality includes maximum sliding friction power, sliding friction work, speed stability time and impact degree.

(1) Maximum sliding power y_1: The maximum sliding power generated during the clutch sliding process.

$$y_1 = \frac{da}{dt} = \frac{d^2v}{dt^2} = \frac{1}{\delta m} \frac{\eta i_g i_0}{r} \frac{dT_{cl}}{dt} \qquad (8)$$

where δ is the rotational mass conversion coefficient of the power shift tractor; η is the transmission efficiency; i_g is the transmission ratio of the gearbox, i_0 is the total transmission ratio of the main reducer and the wheel reducer; T_{cl} is the torque transmitted by the clutch.

(2) Friction power y_2: During the clutch engagement process, there is a speed difference between the master and slave parts, resulting in energy consumption. The generation of sliding friction work will make the friction material on the surface of the friction plate wear and reduce the torque transmission performance of the clutch.

$$y_2 = \int_{t0}^{t1} T_c(\omega_e - \omega_c)dt \qquad (9)$$

In the formula, t_0 is the moment when the clutch produces torque, and t_1 is the moment when the clutch is fully combined to eliminate the speed difference.

(3) Speed stability time y_3: When the power shift tractor reaches the target speed, it is determined that the power shift tractor starts to complete, and the time period when the clutch starts to fill oil to no speed difference is defined as the speed stability time.

(4) Impact degree y_4: the change rate of longitudinal acceleration of a power shift tractor. The greater the impact value, the stronger the sudden frustration of the power shift tractor.

$$y_4 = \max(T_c(\omega_e - \omega_c)) \tag{10}$$

The throttle opening and the throttle opening change rate are the driver's actions, representing the driver's starting intention; the longitudinal acceleration of the vehicle represents the reaction of the tractor to the driver's action. It is reasonable to combine the driver's subjective intention and the tractor's response to start the control. The fuzzy identification system is used to determine the weight of the four clutch engagement quality indicators in the comprehensive evaluation index (Figure 5).
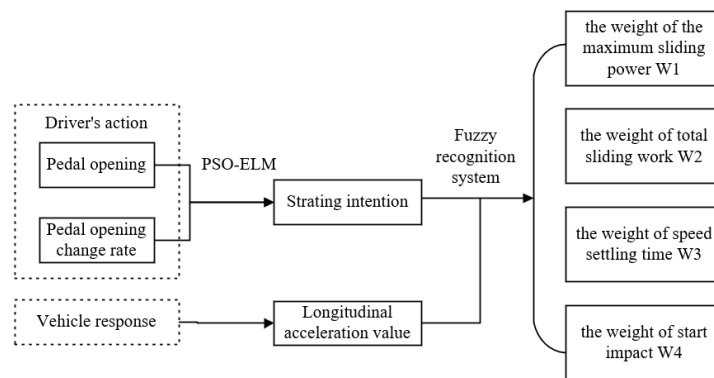

Figure 5. W1–W4 determination method flow chart.

The weight fuzzy identification process [39] is as follows: The fuzzy linguistic variables of the driver's intention are selected as {negative large, negative small, zero, positive small, positive large}, the corresponding fuzzy subsets are {NB, NS, ZE, PS, PB}, and the domain is [–6, 6]; The fuzzy linguistic variables of the driver's intention are selected as {negative large, negative small, zero, positive small, positive large}. The fuzzy linguistic variable of longitudinal acceleration is selected as {small, medium and large}, and the domain is [–6, 6]. The four weight fuzzy linguistic variables are selected as {small, medium and large}, and the domain is [0, 1]; The membership function selects the triangle membership function. The formulation of fuzzy control rules. The weight values of the maximum sliding friction power, sliding friction work, vehicle speed stabilization time and impact degree are shown in Figure 6.
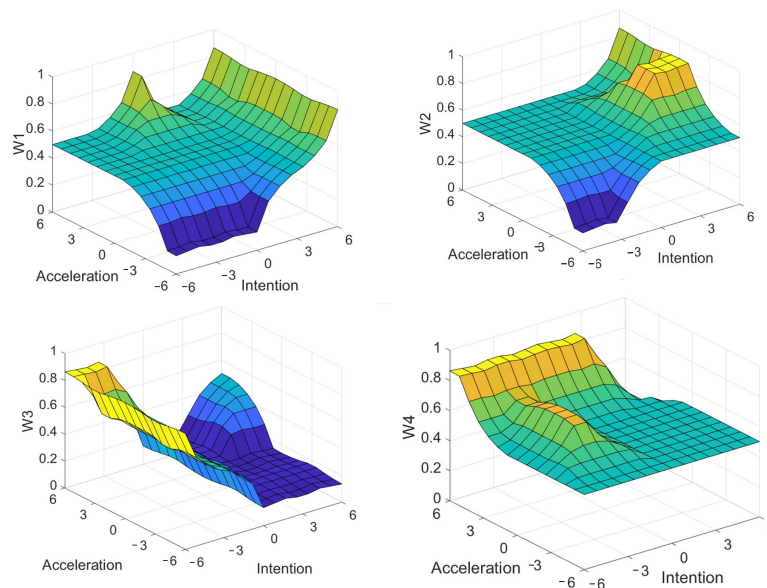

Figure 6. W1–W4 value.

2.3.2. Establishment of Starting Clutch Control Strategy Knowledge Base

The wet clutch control strategy knowledge base is established based on the wet clutch test bench (Figure 7), which was independently developed by the research group [40], and the SimulationX wet clutch engagement quality simulation test platform.

Figure 7. Wet clutch test bench. 1—hydraulic control station. 2—eddy current dynamometer. 3—drive shaft. 4—wet clutch box. 5—speed torque sensor. 6—motor.

The establishment steps of the wet clutch control strategy knowledge base are as follows:
① Through the wet clutch test bench, 20 sets of clutch oil pressure curves are obtained.
② The engagement quality of wet clutch under 20 control strategies is explored on the clutch engagement quality simulation platform, and the knowledge base of clutch control strategy is formed.

a.   Bench test of starting clutch

The variable frequency speed-regulating motor (YXVF315L2-4 type, produced by Anhui Wannan Motor Co., Ltd., Wannan, China) is used as the power source of the test bench. The rated torque is 1286 Nm, and the speed range is 0–1450 r/min. The output power of the motor is adjusted by the Delixi frequency converter so as to change the speed of the input end of the wet clutch. A speed and torque sensor (ZJ-2000A, Jiangsu Lanling Electromechanical Technology Co., Ltd., Nantong, China) is installed on the driving shaft of the wet clutch box. The speed range is 0–3000 r/min, and the torque range is 0.01–2000 Nm. An eddy current dynamometer (CW2000B, Jiangsu Lanling Electromechanical Technology Co., Ltd., Nantong, China) was installed at the output end of the wet clutch box to simulate the load at the output shaft end of the clutch and integrate a speed and torque sensor. The hydraulic control station of the clutch mainly includes the main oil relief valve, the proportional pressure reducing valve, the oil pressure sensor, the oil pump and the oil pump motor, which are used to control the combination and disconnection of the wet clutch.

b.   Simulation test platform for starting clutch based on SimulationX.

Because of the noise interference of the test bench, the impact degree is increased, and the calculated clutch engagement quality is distorted. Therefore, in this paper, we choose to carry out the engagement quality test on the wet clutch simulation test platform based on SimulationX (Figure 8), (ESI ITI, GmbH, Dresden, Germany) [41–43]. Before that, we first verified the accuracy of the simulation test platform. For these test conditions, the relative error between the simulation results and the test results of the maximum output speed of the gearbox is 5.3%, which verifies the correctness of the simulation model. The working condition of the test is that a power shift tractor (8.5 t) runs on the ground without hanging agricultural machinery. And the engine speed is 1070 r/min (engine minimum stable speed), and the load is 85.17 Nm.
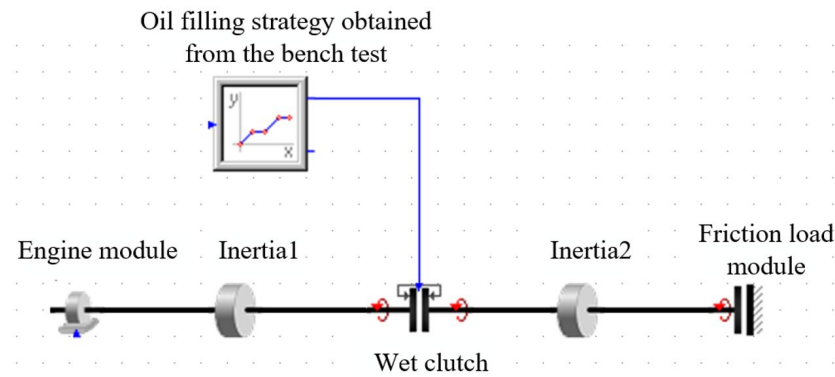
Figure 8. Wet clutch engagement quality simulation test platform.

2.3.3. Establishment of Comprehensive Evaluation Index for Starting under Different Driver Intentions

In order to eliminate the influence of the order of magnitude of different indicators on the final results, the data should be first normalized and substituted into the overall evaluation function of the starting quality to calculate (Figure 9).

$$F = [y_1, y_2, y_3, y_4], \ \min F = W_1 y_1 + W_2 y_2 + W_3 y_3 + W_4 y_4 \tag{11}$$
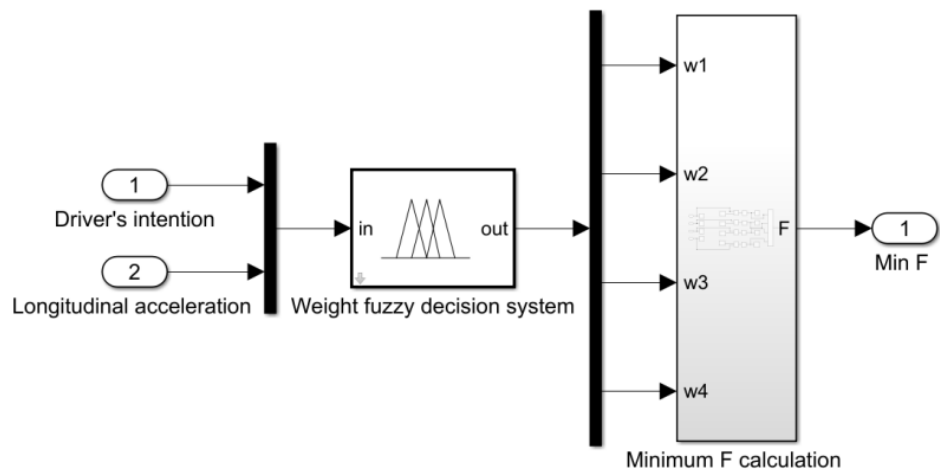

Figure 9. Total evaluation function calculation process.

The comprehensive evaluation index values corresponding to each strategy are calculated, and the clutch control strategy corresponding to the minimum value is the optimal control strategy under the current driver's intention.

2.4. Start-Up Control Simulation Platform Establishment

2.4.1. Design of MPC Controller for Starting Clutch

The mechanism of model predictive control is to predict the future output of the system according to the prediction model at each sampling time of the system and to correct the prediction model according to the current actual measured system output. The open-loop optimization problem in a certain time domain is solved online, and the first element of the obtained control sequence is applied to the controlled object. At the next sampling time, the above process is repeated to re-solve [44–46].

In this paper, a PST starting clutch oil pressure controller is designed based on the model predictive controller. The control goal is to achieve precise control of the clutch oil

pressure [47]. The incremental form of the controller model is derived. The state space model is discretized to obtain a discrete incremental state space model:

$$
\begin{cases}
\triangle x(k+1) = A \triangle x(k) + B_u \triangle u(k) + B_d \triangle d(k) \\
y_c(k) = C_c \triangle x(k) + y_c(k-1)
\end{cases}
\tag{12}
$$

In the formula:

$$
\begin{cases}
\triangle x(k) = x(k) - x(k-1) \\
\triangle u(k) = u(k) - u(k-1) \\
\triangle d(k) = d(k) - d(k-1)
\end{cases}
\tag{13}
$$

$x(k)$ is a state variable, $u(k)$ is a control input, $d(k)$ is a measurable interference input, $y_c(k)$ is the controlled output. The optimization problem can be described as:

$$
J = \left\| T_y (Y_p(k+1|k) - R_e(k+1)) \right\|^2 + \left\| T_u \triangle U(k) \right\|^2
\tag{14}
$$

In the formula, $Y_p(k+1|k)$ is the predictive output, $\triangle U(k)$ is the control increment sequence, $R_e(k+1)$ is the given input, m and p is the control time domain and prediction time domain.

$$
Y_p(k+1|k) = \begin{bmatrix} y(k+1|k) \\ y(k+2|k) \\ \vdots \\ y(k+p|k) \end{bmatrix}, \triangle U(k) = \begin{bmatrix} \triangle u(k) \\ \triangle u(k+1) \\ \vdots \\ \triangle u(k+m-1) \end{bmatrix}, R_e(k+1) = \begin{bmatrix} r(k+1) \\ r(k+2) \\ \vdots \\ r(k+p) \end{bmatrix}
\tag{15}
$$

And,

$$
y(k+i|k) = [\Delta \omega(k+i|k)]
\tag{16}
$$

$$
\triangle u(k+i|k) = \begin{bmatrix} \Delta T_e(k+i|k) \\ \Delta \dot{T}_c(k+i|k) \end{bmatrix}
\tag{17}
$$

$$
r(k+i) = \Delta \omega_{\text{ref}}(k+i|k)
\tag{18}
$$

The weighting matrix are:

$$
T_y = \begin{bmatrix} \gamma_{y,1} & 0 & \cdots & 0 \\ 0 & \gamma_{y,2} & \cdots & 0 \\ \vdots & \vdots & \vdots & \vdots \\ 0 & 0 & \cdots & \gamma_{y,p} \end{bmatrix}, T_u = \begin{bmatrix} \gamma_{u,1} & 0 & \cdots & 0 \\ 0 & \gamma_{u,2} & \cdots & 0 \\ \vdots & \vdots & \vdots & \vdots \\ 0 & 0 & \cdots & \gamma_{u,m} \end{bmatrix}
\tag{19}
$$

And

$$
\gamma_{u,i} = \begin{bmatrix} \gamma_{T_e,i} & 0 \\ 0 & \gamma_{\dot{T}_c,i} \end{bmatrix}
\tag{20}
$$

T_y is the weight factor of the output sequence. The larger the value is, the smaller the error of clutch oil pressure tracking is. T_u is the weight factor of the control signal. The larger the value, the smaller the cost and the smaller the consumption when the controller moves. T_y and T_u are mutually restricted, so it is necessary to coordinate these two values according to the control requirements in the actual system.

The constraint conditions are:

$$
u_{\min}(k+i) \leq u(k+i) \leq u_{\max}(k+i), \; i = 0, 1, \ldots, m-1
\tag{21}
$$

$$
\triangle u_{\min}(k+i) \leq \triangle u(k+i) \leq \triangle u_{\max}(k+i), \; i = 0, 1, \ldots, m-1
\tag{22}
$$

$$
y_{c\,\min}(k+i) \leq y_c(k+i) \leq y_{c\,\max}(k+i), \; i = 0, 1, \ldots, p
\tag{23}
$$

The optimal control sequence is obtained by solving, and the optimization results are applied to the system.

$$\triangle U(k) = [\triangle u(k), \triangle u(k+1), \dots, \triangle u(k+m-1)] \tag{24}$$

According to the analysis of the starting process and the starting control strategy of the power shift tractor, the speed differences between the clutch $\Delta\omega$ and the clutch and the torque transmitted by the clutch T_{cl} are selected as the state variables, and the first derivative of the torque transmitted by the clutch is taken as the control variable. The state space equation of the PST starting process is:

$$\begin{cases} \dot{x} = Ax + Bu + D \\ y = Cx \end{cases} \tag{25}$$

Among them, $A = \begin{bmatrix} 0 & -(\frac{1}{I_e} + \frac{1}{I_0}) \\ 0 & 0 \end{bmatrix}, B = \begin{bmatrix} 0 \\ 1 \end{bmatrix}, C = \begin{bmatrix} 1 & 0 \end{bmatrix}, D = \begin{bmatrix} \frac{i_1}{I_e}T_e + \frac{1}{i_v i_0 I_c}T_f \\ 0 \end{bmatrix},$

$x = [\Delta\omega, T_{cl}]$, $u = \dot{T}_{cl}$, $\Delta\omega = \omega_e - \omega_c$. ω_e is the speed of the active end of the clutch, ω_c is the speed of the driven end of the clutch. I_e is the equivalent rotational inertia of the active end of the clutch, I_0 is the equivalent rotational inertia of the clutch driven end, i_1 is the transmission ratio of PST starting section, T_e is the output torque of the engine, I_c is the equivalent rotational inertia of the whole machine, $i_v i_0$ is the transmission ratio of the central drive and the final drive, T_f is the resistance moment.

According to the principle of model predictive control, the Formula (25) is discretized and rewritten into an augmented format. The discretization step size = 0.05 s, and the predictive model of starting clutch control is obtained as follows:

$$\begin{cases} x(k+1) = A_1 x(k) + B_1 u(k) + D_1 \\ y = C_1 x(k) \end{cases} \tag{26}$$

Among them,

$$A1 = \begin{bmatrix} 1 & -(\frac{\Delta t}{I_e} + \frac{\Delta t}{I_0}) \\ 0 & 1 \end{bmatrix}, B1 = \begin{bmatrix} 0 \\ \Delta t \end{bmatrix}, C1 = \begin{bmatrix} 1 & 0 \end{bmatrix}, D1 = \begin{bmatrix} \frac{i_1 \Delta t}{I_e}T_e + \frac{\Delta t}{i_v i_0 I_c}T_f \\ 0 \end{bmatrix}$$

When the PST tractor starts, it is necessary to ensure that the oil-filling process of the wet clutch is consistent with the target process as much as possible, and the change range of the control quantity cannot be too large. The objective function of the controller is set as follows:

$$\begin{cases} \min_{\Delta u(k)} J = J_1 + J_2 \\ J_1 = \|y(k+1) - R(k+1)\|^2 \\ J_2 = \|\Delta u(k)\|^2 \end{cases} \tag{27}$$

Among them, $y(k+1)$ is the prediction oil pressure (MPa); $R(k+1)$ is oil pressure target trajectory.

When the PST tractor starts, the change of the oil filling pressure is too fast to produce the starting impact. The constraint condition of the controller is set to:

$$\Delta u_{\min}(k) \leq \Delta u(k) \leq \Delta u_{\max}(k), \forall k \geq 0 \tag{28}$$

According to the prediction model, objective function and constraint conditions, the MPC tracking controller of the starting clutch is designed as follows (Figure 10):

The oil pressure tracking control flow is as follows: The system's current state error is input into the system error model, and the system's predicted output can be obtained. After the solution of the objective function is completed in each control cycle, the control

error increment sequence is obtained. The first amount in the control sequence is used as the actual control error increment of the system at the current time. The control error at the current time can be obtained by combining the control error at the previous time, and then the reference control amount is corrected to obtain the current actual control amount, $u(k)$.
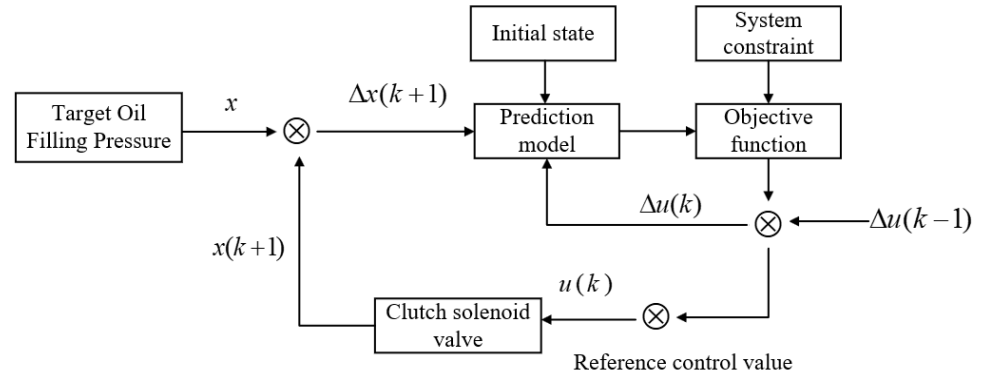

Figure 10. Oil pressure tracking control based on MPC.

2.4.2. Construction of Starting Simulation Platform for Power Shift Gearbox

The proportional pressure electromagnetic of the starting clutch has strong nonlinearity. In order to simplify the system modeling, this paper studies the following two simplifications: (1) ignore the influence of hydraulic oil leakage during valve movement; (2) the hydraulic pressure of the pressure feedback chamber is approximately equal to the output pressure of the proportional voltage valve; (3) ignore the volume of the proportional hydraulic chamber and the inflow of hydraulic oil flow.

Using AMEsim and Simulink to build a joint simulation platform to simulate and analyze the PST start-up process (Figure 11).
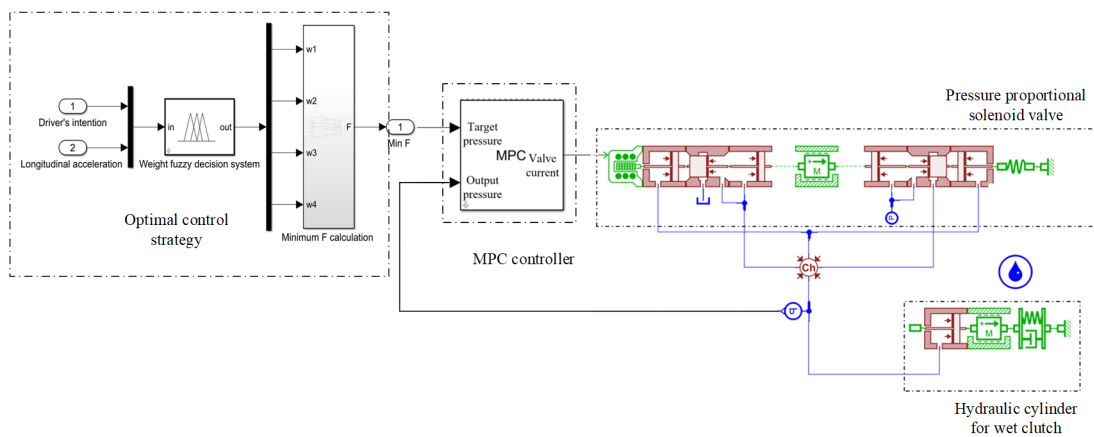

Figure 11. Construction of electronic control simulation platform for starting clutch.

3. Results

3.1. Accuracy Verification and Comparison of PSO-ELM Identification Model for Driver's Starting Intention

From the 60 sets of starting tests, 48 sets of data, including the pedal-opening signal and acceleration signal, were randomly selected as training data, and 12 sets of tests were used as test data. Because of the dimension and order of magnitude of the data, it is difficult to guarantee the accuracy of the trained neural network for the recognition results of the new sample data. Therefore, it is necessary to normalize the data of each node first. The validation data are imported into the trained PSO-ELM identification model.

The experimental resultsshow (Figure 12) that the error between the output value and the true value is less than 0.15, and the circle is an integer value. It can be seen from

Figure 5 that the R2 of the prediction set of the PSO-ELM model is 0.96891, and the R_2 of the ELM model prediction set is 0.91593, indicating that the PSO-ELM model has a better degree of nonlinear fitting. The simulation mean square error mse of the PSO-ELM model is 0.01.
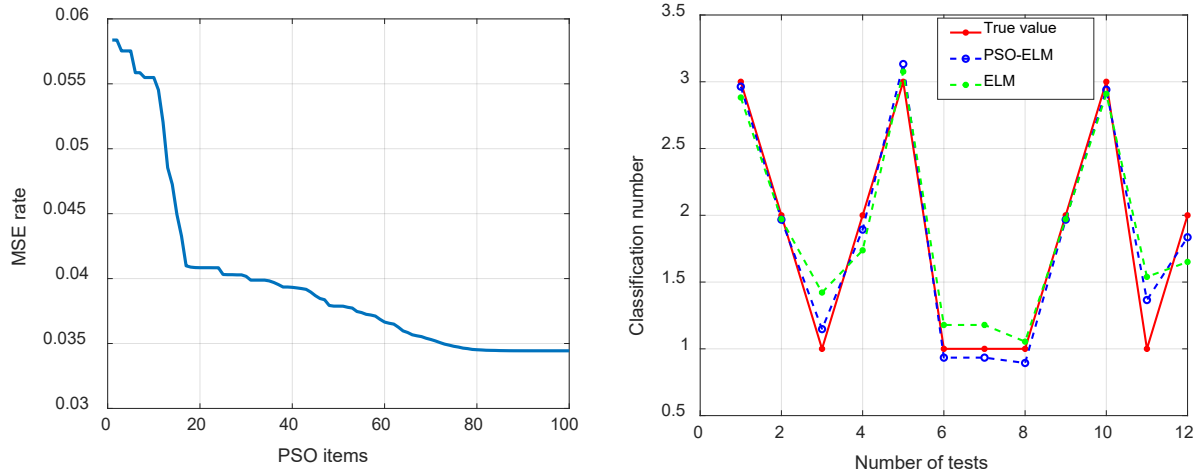

Figure 12. The identification results of ELM and PSO-ELM compared with the real values.

Among the 12 sets of verification data (Table 2), the ELM model correctly identified 6 sets of intentions, and the recognition accuracy was 50%. The PSO-ELM model correctly identified 11 sets of intentions and only one set of errors, and the recognition accuracy was 91.67%, which was 41.67% higher than that of ELM. In driving intention recognition, the PSO-ELM identification model performs better.

Table 2. Comparison of model prediction accuracy.

Test Number	1	2	3	4	5	6	7	8	9	10	11	12
True value	3	2	1	2	3	1	1	1	2	3	1	2
ELM value	3	2	1.42	1.73	3	1.17	1.17	1	2	3	1.54	1.65
PSO-ELM value	3	2	1	2	3	1	1	1	2	3	1	1.83

3.2. Tractor Starting Control Strategy Considering Driver's Intention

3.2.1. Starting Clutch Engagement Oil Pressure Range to Determine the Test Results

It can be seen from the Table 3 that when the clutch oil pressure is less than 1.1 MPa, the clutch is not fully engaged, and the maximum output speed of the gearbox does not reach the theoretical output speed (Figure 13). At this time, the bench will emit obvious abnormal noise, and the speed drop during the speed rise is a sign that the clutch is not fully engaged.

Table 3. The maximum output speed of gearbox under 6 kinds of oil pressure.

Oil Pressure of Wet Clutch/MPa	Maximum Output Speed of the Gearbox/r/min	Theoretical Output Speed/r/min
0.5	128.52	297
0.6	161.09	297
0.7	191.7	297
0.8	225.61	297
0.9	268.82	297
1	293	297

When the oil pressure is greater than 4.9 MPa, the clutch engagement will produce a significant impact during the test, and a large noise will be generated. Figure 14 shows the

oil filling process of the clutch when the oil pressure is 5 MPa. It can be seen from the diagram that the oil pressure rises very fast, and the clutch oil filling process is too fast, which will affect the clutch engagement speed and increase the impact of the clutch engagement.
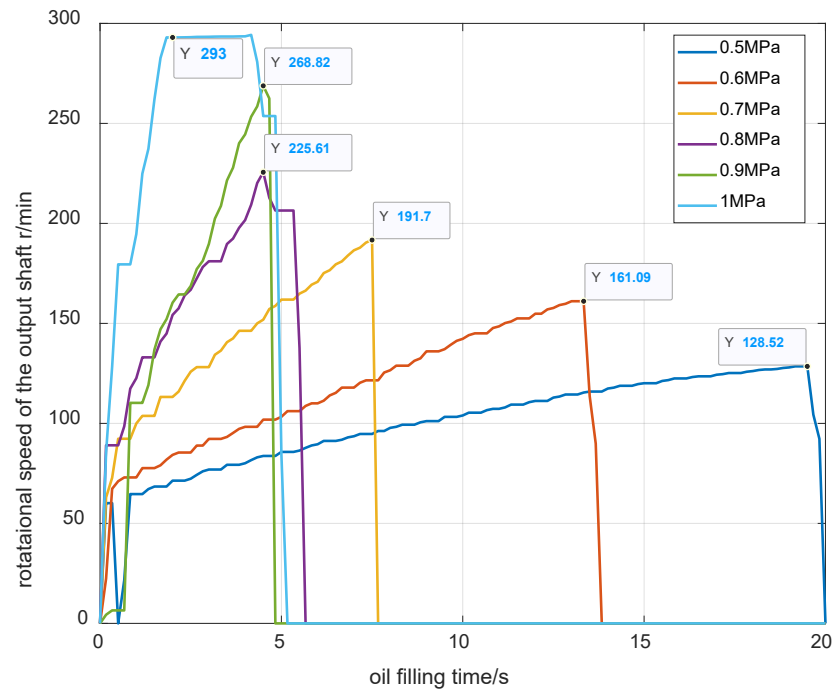

Figure 13. The output speed change curve of gearbox under 6 kinds of oil pressure.
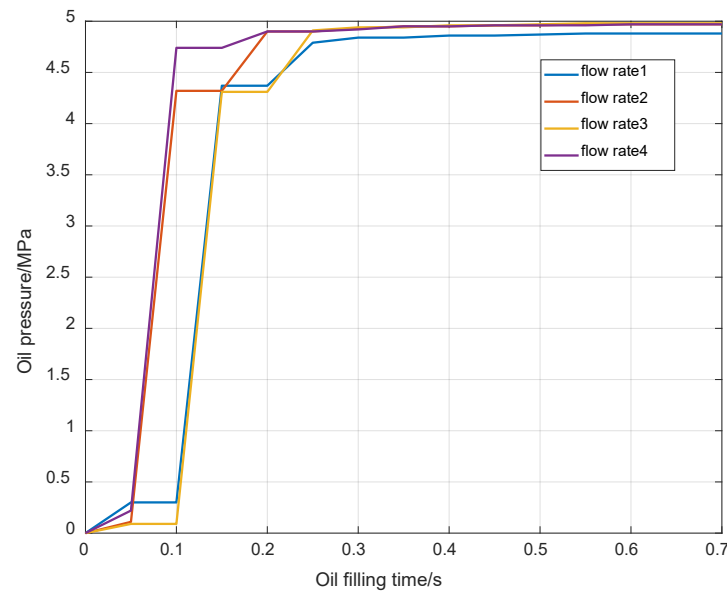

Figure 14. Five megapascals oil pressure change curve of clutch.

Therefore, in this paper, the range of oil filling pressure is set to 1.1–4.9 MPa when establishing the knowledge base of starting clutch control strategy. In the process of a single test, the opening of the flow valve is first adjusted, and then the oil filling pressure of the clutch is set in the host computer to record the change in the oil filling pressure of the clutch with time. By changing the oil filling pressure (1.1, 2.1, 3.1, 4.1, 4.9 MPa) and the opening of the flow valve (30%, 50%, 70%, 90%), 20 sets of clutch oil filling strategies are obtained (Figure 15 is the clutch oil filling control strategy of 1.1 MPa and 2.1 MPa).
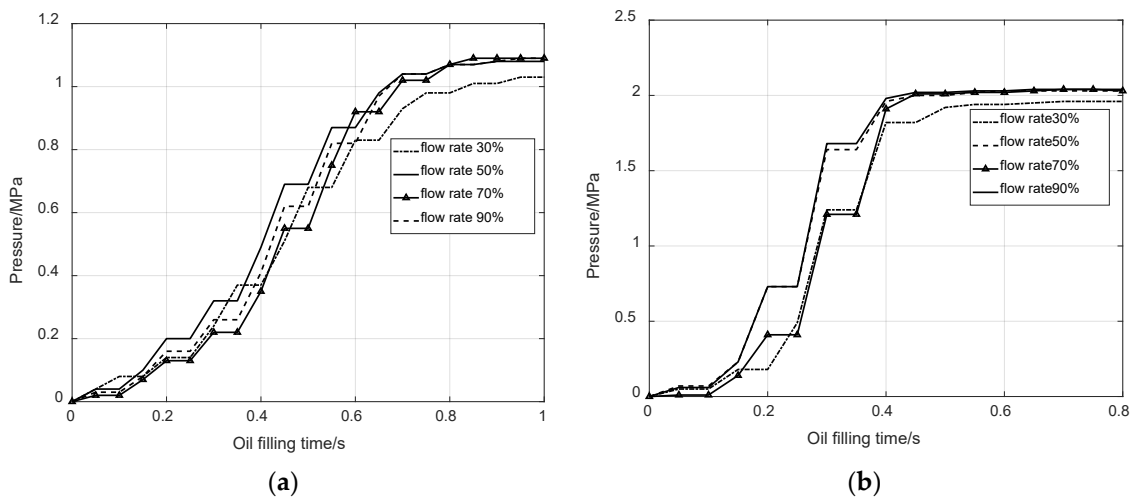
Figure 15. Wet clutch oil filling control strategy. (**a**) 1.1 MPa; (**b**) 2.1 MPa.

3.2.2. Accuracy Verification Results of Wet Clutch Simulation Test Platform

Simulation test platform for starting clutch based on SimulationX: Because of the noise interference of the test bench, the impact degree is increased, and the calculated clutch engagement quality is distorted. Therefore, in this paper, we choose to carry out the engagement quality test on the wet clutch simulation test platform based on SimulationX (ESI ITI, GmbH, Germany) [1–3]. Before that, we first verified the accuracy of the simulation test platform. For these test conditions, the relative error between the simulation results and the test results of the maximum output speed of the gearbox is 5.3%, which verifies the correctness of the simulation model (Figure 16).
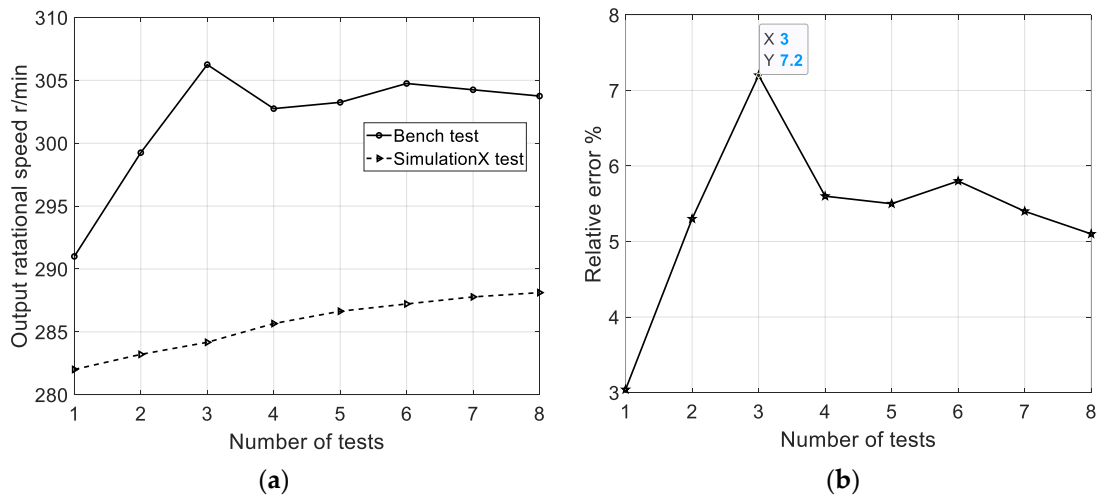

Figure 16. The simulation platform is compared with the test bench to verify the results. (**a**) Simulation output speed and bench test output speed; (**b**) Relative error.

The working condition of the test is that a certain type of power shift tractor (8.5 t) runs on the ground without hanging agricultural machinery, and the engine speed is 1070 r/min (engine minimum stable speed) and load is 85.17 Nm.

3.2.3. The Knowledge Base of Tractor Starting Clutch Control Strategy

Through the clutch simulation test platform, the knowledge base of the starting clutch control strategy is obtained, as shown in Table 4:

Table 4. Starting clutch control strategy knowledge base.

Test Number	Oil Pressure/MPa	Flow Valve Opening%	Maximum Sliding Power J	Friction Power J	Speed Stability Time s	Impact m/s^3
1	1.1	0.3	575,489.94	56,400.61	0.20	584,899.50
2	1.1	0.5	755,803.53	57,981.71	0.25	937,238.46
3	1.1	0.7	981,585.26	55,403.02	0.38	1,258,678.03
4	1.1	0.9	698,689.29	60,328.37	0.31	1,090,579.35
5	2.1	0.3	833,068.79	49,755.37	0.18	1,064,541.15
6	2.1	0.5	888,340.15	36,262.43	0.12	1,446,325.92
7	2.1	0.7	1,022,171.96	38,896.36	0.17	1,624,146.11
8	2.1	0.9	964,428.49	36,996.41	0.13	1,273,260.25
9	3.1	0.3	1,665,466.82	36,756.97	0.14	1,986,833.58
10	3.1	0.5	379,151.35	35,698.86	0.11	598,887.57
11	3.1	0.7	1,222,831.56	33,686.07	0.12	1,685,159.26
12	3.1	0.9	546,644.01	19,182.57	0.06	543,346.56
13	4.1	0.3	835,046.18	21,643.97	0.06	1,080,757.57
14	4.1	0.5	379,151.35	35,698.86	0.11	598,887.57
15	4.1	0.7	417,575.59	24,198.42	0.06	681,833.18
16	4.1	0.9	325,316.41	6429.21	0.07	504,150.58
17	4.9	0.3	829,032.18	68,997.07	0.24	1,066,653.49
18	4.9	0.5	806,755.85	60,128.87	0.28	1,084,836.86
19	4.9	0.7	379,151.35	4798.62	0.02	535,396.52
20	4.9	0.9	474,832.52	45,256.81	0.11	751,212.03

3.3. Verification of Starting Clutch Control Effect Based on MPC Controller

Taking the step signal within 100 s of sampling time as the target value, the control effect of the starting clutch MPC controller is verified.

4. Discussion

(1) According to the comparison of the identification results of the two identification methods in Table 2, it can be found that the prediction simulation error of the PSO-ELM model is 38.05% lower than that of the ELM model. Among them, with the help of the PSO algorithm in the multi-dimensional solution space, a large number of random particles will search for the position of the current optimal particle and then update their speed and position to achieve the goal of quickly finding the optimal solution to the problem. The PSO-ELM identification model can avoid the network falling into the local optimum and find the global optimal model parameter solution, thereby improving the accuracy of the model. Compared with the unoptimized ELM, the PSO-ELM identification model has a better identification effect on the identification of the driver's starting intention.

(2) In Figure 17, it can be seen that the MPC controller can better follow the target value. There is a certain tracking error in the initial stage of control, and the tracking error decreases rapidly in the later stage, and the oil pressure output value is stabilized at the target value. On the simulation experiment platform, the starting quality of the starting control strategy determined by the PSO-ELM-fuzzy weight method and the conventional starting control strategy is compared.

By using the PSO-ELM-fuzzy weight starting control strategy (Table 5), compared with the linear control strategy, the maximum sliding friction power y1 is reduced by 45%, the sliding friction power is reduced by 69.45%, the speed stabilization time is shortened by 0.11 s, and the impact degree is increased by 0.003%. Compared with the linear control strategy, the starting control strategy proposed in this paper takes the driver's intention as one of the important criteria for the formulation of the starting control strategy. For different driver intentions, the optimal starting control strategy under the current intention is proposed. In summary, the PSO-ELM-fuzzy weight starting control strategy proposed in this paper has better starting quality.
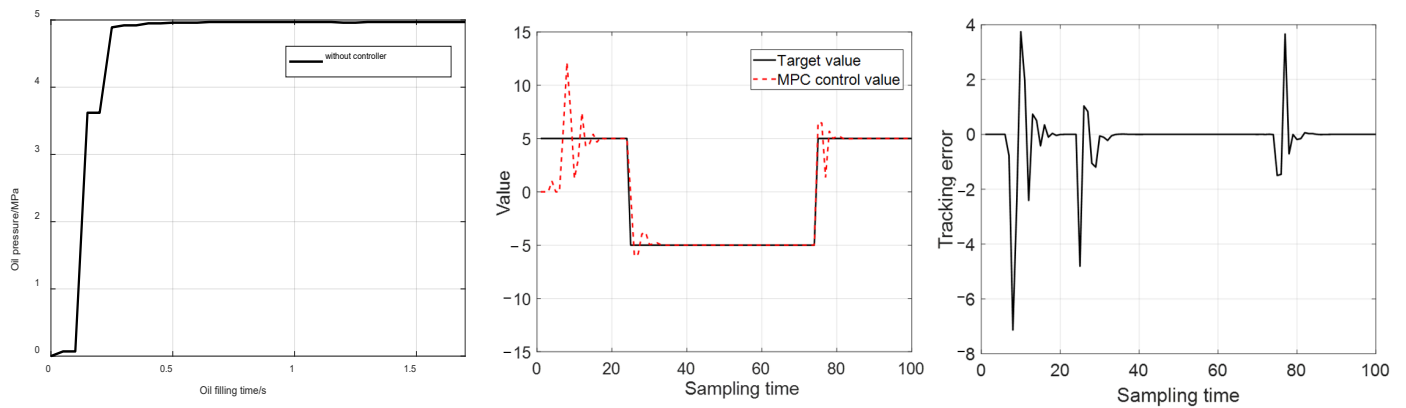
Figure 17. MPC controller square wave signal tracking control.

Table 5. Comparison between PSO-ELM-fuzzy weight starting strategy and linear control strategy.

Content	Maximum Sliding Power J	Friction Power J	Speed Stability Time s	Impact m/s³
PSO-ELM-fuzzy weight starting strategy	417,575.59	24,198.42	0.06	681,833.18
Linear control strategy	762,047.30	79,213.59	0.17	679,402.27

5. Conclusions

In this paper, aiming at the starting quality of a power shift tractor, a tractor starting control strategy considering the driver's intention is proposed. Firstly, the identification modeling data samples of the driver's starting intention are obtained by vehicle testing. After the driver's intention identification model is established, we match the optimal control strategy for different starting intentions. Therefore, we establish a knowledge base for starting control strategies through the joint bench test and simulation test platform. After the establishment of the control strategy knowledge base and the driver's intention identification model, we chose the fuzzy weight method to determine the connection between the driver's intention and the control strategy. At the same time, the MPC starting controller of the power shift gearbox is established to verify the control effect of the starting control strategy proposed in this paper. The following conclusions are drawn from this study:

(1) The ELM driver intention identification model improved by the PSO algorithm has a prediction accuracy of 91.67%. Compared with the ELM identification model, the prediction accuracy is improved by 41.67%, and the ELM model optimized by PSO can avoid the network falling into local optimum.

(2) The wet clutch has a minimum oil filling threshold and a maximum oil filling threshold. The minimum oil filling threshold is determined by the structural size and working condition of the wet clutch, and the clutch has sliding friction when the value is less than this value. The maximum oil filling threshold can be obtained from the test. If the value is greater than this value, the clutch engagement speed is too fast, resulting in a large impact and poor engagement quality. Through experiments, the oil filling pressure range of the wet clutch studied in this paper is 1.1 MPa–4.9 MPa.

(3) Compared with the linear control strategy, the maximum sliding friction power is reduced by 45%, and the sliding friction power is reduced by 69.45%. The speed stabilization time is shortened by 0.11 s, and the impact degree is in-creased by 0.003%. In summary, the PSO-ELM-fuzzy weight starting strategy proposed in this paper has better starting quality.

This paper studies the starting process of power shift tractors from the perspective of 'people–vehicle–ground'. It is expected to improve the starting quality of power shift tractors, improve the working environment of tractor drivers, and protect their physical

and mental health. At the same time, it is expected to provide research help for tractors to realize intelligent automatic driving.

References

1. Mairghany, M.; Yahya, A.; Adam, N.M.; Mat Su, A.; Aimrun, W.; Elsoragaby, S. Rotary tillage effects on some selected physical properties of fine textured soil in wetland rice cultivation in Malaysia. *Soil Tillage Res.* **2019**, *194*, 104318. [CrossRef]
2. AI-Sager, S.M.; Almady, S.S.; Marey, S.A.; AI-Hamed, S.; Aboukarima, A.M. Prediction of specific fuel consumption of a tractor during the tillage process using an artificial neural network method. *Agronomy* **2024**, *14*, 492. [CrossRef]
3. Vu, N.-L.; Messier, P.; Nguyễn, B.-H.; Vo-Duy, T.; Trovão, J.; Desrochers, A.; Rodrigues, A. Energy-optimization design and management strategy for hybrid electric non-road mobile machinery: A case study of snowblower. *Energy* **2023**, *284*, 129249. [CrossRef]
4. Mederle, M.; Urban, A.; Fischer, H.; Hufnagel, U.; Bernhardt, H. Optimization potential of a standard tractor in road transportation. *Landtechnik* **2015**, *70*, 194–202.
5. Zhou, X.Y.; Qin, D.T.; Hu, J. Multi-objective optimization design and performance evaluation for plug-in hybrid electric vehicle powertrains. *Appl. Energy* **2017**, *208*, 1608–1625. [CrossRef]
6. Mattetti, M.; Maraldi, M.; Sedoni, E.; Molari, G. Optimal criteria for durability test of stepped transmissions of agricultural tractors. *Biosyst. Eng.* **2019**, *100*, 145–155. [CrossRef]
7. Molari, G.; Sedoni, E. Experimental evaluation of power losses in a power-shift agricultural tractor transmission. *Biosyst. Eng.* **2008**, *100*, 177–183. [CrossRef]
8. Savaresi, S.M.; Taroni, F.L.; Predivi, F.; Bittaniti, S. Control system design on a power-split CVT for high-power agricultural tractors. *IEEE-ASME Trans. Mechatron.* **2004**, *9*, 569–579. [CrossRef]
9. Xia, Y.; Sun, D.Y.; Qin, D.T.; Zhou, X.Y. Optimization of the power-cycle hydro-mechanical parameters in a continuously variable transmission designed for agricultural tractors. *Biosyst. Eng.* **2020**, *193*, 12–24. [CrossRef]
10. Macor, A.; Rossetti, A. Optimization of hydro-mechanical power split transmissions. *Mech. Mach. Theory* **2011**, *46*, 1901–1919. [CrossRef]
11. Cheng, Z. High nonlinearity of BEV's stepped automatic transmission design objectives and its optimal solution by a novel ISA-RSA. *Energy* **2023**, *282*, 128834. [CrossRef]
12. Tanelli, M.; Panzani, G.; Savaresi, S.M.; Pirla, C. Transmission control for power-shift agricultural tractors: Design and end-of-line automatic tuning. *Mechatronics* **2011**, *21*, 285–297. [CrossRef]
13. Kim, D.C.; Kim, K.U.; Park, Y.J.; Huh, J.Y. Analysis of shifting performance of power shuttle transmission. *J. Terramechanics* **2007**, *44*, 111–122. [CrossRef]
14. Raikwar, S.; Tewari, V.K.; Mukhopadhyay, S.; Verma, C.R.B.; Rao, M.S. Simulation of components of a power shuttle transmission system for an agricultural tractor. *Comput. Electron. Agric.* **2015**, *114*, 114–124. [CrossRef]
15. Sun, C.Y.; Si, T.F.; Zhu, M.H.; Han, M.Y.; Hou, Z.H.; Zhang, Z.J. Research on the optimization of power shift quality based on the oil pressure segment control strategy of wet clutch. *J. Chin. Agric. Mech.* **2022**, *43*, 106–112.
16. Ouyang, T.C.; Li, S.Y.; Huang, F.; Zhou, F.; Chen, N. Mathematical modeling and performance prediction of a clutch actuator for heavy-duty automatic transmission vehicles. *Mech. Mach. Theory* **2019**, *136*, 190–205. [CrossRef]
17. Balau, A.E.; Caruntu, C.F.; Lazar, C. Simulation and control of an electro-hydraulic actuated clutch. *Mech. Syst. Signal Process.* **2011**, *25*, 1911–1922. [CrossRef]

18. Zeng, X.H.; Chen, H.X.; Dong, B.B.; Song, D.F. Modeling and Simulation of the Hydraulic Actuator System of Wet Clutch. *Mach. Tool Hydraul.* **2021**, *49*, 120–125.
19. Wu, J.P.; Wang, L.Y.; Li, L.; Zhou, Q.J. The study on the influence of control signal on charge characteristics of wet clutch. *Chin. Hydraul. Pneum.* **2016**, *02*, 62–66.
20. Benloucif, A.; Nguyen, A.T.; Sentouh, C.; Popieul, J.C. Cooperative trajectory planning for haptic shared control between driver and automation in highway driving. *IEEE Trans. Ind. Electron.* **2019**, *66*, 9846–9857. [CrossRef]
21. Marcano, M.; Díaz, S.; Pérez, J.; Irigoyen, E. A review of shared control for automated vehicles: Theory and applications. *IEEE Trans. Hum. Mach. Syst.* **2020**, *50*, 475–491. [CrossRef]
22. Li, M.J.; Cao, H.T.; Song, X.L.; Huang, Y.J.; Wang, J.Q.; Huang, Z. Shared control driver assistance system based on driving intention and situation assessment. *IEEE Trans. Ind. Inform.* **2018**, *14*, 4982–4994. [CrossRef]
23. Huang, T.; Fu, R.; Sun, Q.Y.; Deng, Z.J.; Liu, Z.F.; Jin, L.S.; Khajepour, A. Driver lane change intention prediction based on topological graph constructed by driver behaviors and traffic context for human-machine co-driving system. *Transp. Res. Part C Emerg. Technol.* **2024**, *160*, 104497. [CrossRef]
24. Liu, Z.Q.; Wu, X.G.; Ni, G.; Zhang, T. Driving intention recognition based on HMM and SVM cascade algorithm. *Automot. Eng.* **2018**, *40*, 858–864.
25. Wang, Q.L.; Tang, X.Z.; Wang, P.Y.; Tian, L.Y.; Sun, L. Driving intention identification method for hybrid vehicles based on Neural Network. *Trans. Chin. Soc. Agric. Mach.* **2012**, *43*, 32–36.
26. Hong, W.C.H.; Dong, Y.C.; Zheng, F.F.; Wei, S.Y. Hybrid evolutionary algorithms in a SVR traffic flow forecasting model. *Appl. Math. Comput.* **2011**, *217*, 6733–6747. [CrossRef]
27. Yao, Y.; Zhao, X.H.; Wu, Y.P.; Zhang, Y.L.; Rong, J. Clustering driving behavior using dynamic time warping and hidden Markov model. *J. Intell. Transp. Syst.* **2019**, *25*, 249–262. [CrossRef]
28. Wang, X.; Guo, Y.; Bai, C. Driver's intention identification with the involvement of emotional factors in two-lane roads. *IEEE Trans. Intell. Transp. Syst.* **2020**, *22*, 6866–6874. [CrossRef]
29. Xie, F.; Lou, J.T.; Zhao, K. A research on vehicle trajectory prediction method based on behavior recognition and curvature constraints. *Automot. Eng.* **2019**, *41*, 1036–1042.
30. Lethaus, F.; Baumann, M.; Koester, F. A comparison of selected simple supervised learning algorithm to predict driver intent based on gaze data. *Neurocomputing* **2013**, *121*, 108–130. [CrossRef]
31. Zhang, L.J.; Tang, X.; Meng, J.D. Driver's head and face visual feature extraction for driving intention recognition. *Automob. Technol.* **2019**, *521*, 18–24.
32. Deng, Q.; Wang, J.; Hillebrand, K. Prediction performance of lane changing behaviors: A study of combining environmental and eye-tracking data in a driving simulator. *IEEE Trans. Interlligent Syst.* **2019**, *21*, 3561–3570. [CrossRef]
33. He, F.; Zhang, X.X.; Chen, W.R. Fault diagnosis method of PEMFC system based on P-L dual feature extraction. *Acta Energiae Solaris Sin.* **2024**, *45*, 492–499.
34. Huang, M.T.; Xing, F.F.; Chen, X.B.; Lu, M. Short-term PV power prediction based on K-means clustering and extreme learning machine combination algorithm. *Water Resour. Power* **2024**, *42*, 216–220.
35. Liu, Y.D.; Ma, J.H.; Wang, X.G. H-beam steel structure prediction expert system based on ELM. *Forg. Stamp. Technol.* **2024**, *49*, 241–248.
36. Sevim, S.Y.; Mladen, T. Estimation of daily potato crop evapotranspiration using three different machine learning algorithms and four scenarios of available meteorological data. *Agric. Water Manag.* **2022**, *228*, 105875.
37. Yam, K.; Ji, Z.; Lu, H. Fast and accurate classification of time series data using extended ELM: Application in fault diagnosis of air handling units. *IEEE Trans. Syst. Man Cybern. Syst.* **2017**, *49*, 1349–1356.
38. Liu, X.; Fan, X.; Guo, Y. Multi-objective optimization of GFRP injection molding process parameters, using GA-ELM, MOFA, and GRA-TOPSIS. *Trans. Can. Soc. Mech. Eng.* **2021**, *46*, 37–49. [CrossRef]
39. Meng, F.; Chen, H.Y.; Zhang, T.; Zhu, X.Y. Clutch fill control of an automatic transmission for heavy-duty vehicle applications. *Mech. Syst. Signal Process.* **2015**, *64–65*, 16–28. [CrossRef]
40. Lu, Z.X.; Wang, Y.T.; Wang, L.; Zhao, Y.R.; Wang, X.W.; Zhou, J.B. Prediction of HMCVT wet clutch friction pair temperature based on IGWPSO-SVM. *Trans. Chin. Soc. Agric. Mach.* **2023**, *54*, 407–415.
41. Kyuhyun, S.; Hwayoung, L.; Jiwon, Y.; Chanho, C.; Sung-Ho, H. Effectiveness evaluation of hydro-pneumatic and semi-active cab suspension for the improvement of ride comfort of agricultural tractors. *J. Terramechanics* **2017**, *69*, 23–32.
42. Savin, V.; Christian, H.; Olav, E.; Ronny, S. Cosimulation of a direct-acting riser-tensioner system—Validation with field measurements and sample simulations. *Ocean. Eng.* **2023**, *276*, 114241.
43. Chen, X.; Chen, F.Q.; Zhou, J.; Li, L.H.; Zhang, Y.L. Cushioning structure optimization of excavator arm cylinder. *Autom. Constr.* **2015**, *53*, 120–130. [CrossRef]
44. Leung, J.; Permenter, F.; Kolmanovsky, I.V. A stability governor for constrained linear–quadratic MPC without terminal constraints. *Automatica* **2024**, *164*, 111650. [CrossRef]
45. Zhang, J.J.; Feng, G.H.; Yan, X.H.; He, Y.D.; Liu, M.N.; Xu, L.Y. Cooperative control method considering efficiency and tracking performance for unmanned hybrid tractor based on rotary tillage prediction. *Energy* **2024**, *288*, 129874. [CrossRef]

46. Robat, A.B.; Arezoo, K.; Alipour, K.; Tarvirdizadeh, B. Dynamics modeling and path following controller of tractor-trailer-wheeled robots considering wheels slip. *ISA Trans.* **2024**, *03*, 004.

47. Xu, Y.T.; Chen, H.; Ji, D.D.; Xu, F. MPC controller design and FPGA implementation for start-up of vehicles. *Control Engineeing China* **2015**, *22*, 785–792.